Experimental section

Materials. Pluronic F127 ($EO_{106}PO_{70}EO_{106}$, Mav = 12600) was purchased from Sigma-Aldrich. Phenol, 0.1 M sodium hydroxide solution, and formaldehyde solution (37 wt%) were bought from Nacalai Tesque. Vulcan XC 72 was purchased from Cabot Corporation.

Preparation for ordered mesoporous polymer (OMP). Ordered mesoporous polymer (OMP) was prepared *via* organic-organic assembly by the following processes. 0.28 g of phenol was first dissolved in 1.05 mL of formaldehyde aqueous solution (37 wt%). Then, 7.5 mL 0.1 M NaOH solution was added and stirred at 70 °C for 30 min. Afterwards, 0.49 g of F127 dissolved in 7.5 mL deionized water was added, and the mixed solution was stirred at 65 °C for 2 h. Subsequently, 25.0 mL of distilled water was added to the mixture and the diluted solution was stirred for another 6 h. 15.0 mL of the obtained solution was transferred in a 100 mL Teflon liner, and then 20.0 mL of water was added dropwise under stirring. The hydrothermal reaction was carried out at 130 °C for 20 h with a ramping rate of 1 °C min^{-1}. The obtained precipitate was washed twice with water and collected by centrifugation. After vacuum drying at 60 °C, rhombic dodecahedral single-crystals were obtained and assigned as OMP.

Preparation for ordered mesoporous carbon (OMC). The as-made OMP single-crystals were carbonized at 900 °C for 2 h under N_2 atmosphere. The ramping rate of the calcination process was 1 °C min^{-1}. The ordered mesoporous carbon was obtained and assigned as OMC.

Preparation for ordered mesoporous nitrogen-doped carbon (OMNC). The ordered mesoporous nitrogen-doped carbon (OMNC) was prepared in a post-synthesis with a direct harsh NH_3 activation. In a typical activation process, 100.0 mg of OMC was put in a quartz boat which was placed in the tube furnace. Firstly, the temperature was increased to the target temperatures (*e.g.*, 800, 900, and 950 °C) with a heating rate of 20 °C min^{-1} under N_2 atmosphere and kept as such for 10 min. Then N_2 was replaced by gaseous NH_3 and kept as such for a certain time period (*e.g.*, 10, 20, and 30 min). The flow rate of NH_3 was 300 mL min^{-1}. NH_3 was then replaced back to N_2 during cooling process. The final product was assigned as OMNC-*T*-*t*, where *T* represents the NH_3 activation temperature and *t* stands for the duration time in minutes.

Characterization. The morphology of the as-prepared single-crystals was analyzed by a field emission scanning electron microscope (FESEM, HITACHI SU-8230) with an accelerating voltage of 5 kV. The mesoporous structure of the as-prepared single-crystals was observed by a transmission electron microscope (TEM, JEOL JEM-2100F) operated at 200 kV. Smallangle X-ray scattering (Rigaku NANO-Viewer) using a camera length of 700 mm was used to evaluate the pore-to-pore distance under a Cu Kα radiation at 40 kV and 30 mA. Nitrogen adsorption-desorption isotherms were obtained by using an AUTOSOB-1 (Quantachrome Instruments, USA). The specific surface area of pristine OMC and OMNC-*T*-*x* was analyzed by Multipoint Brunauer-Emmett-Teller (BET) method. The micropore surface area and micropore volume

were analyzed by *t*-plot method. The pore size distribution was studied by the nonlocal density functional theory (NLDFT) method. The nitrogen content and chemical state of nitrogen were investigated using X-ray photoelectron spectroscopy (PHI Quantera SXM) with Al Kα radiation at 20 kV and 5 mA. The C1s level at 284.5 eV was used to calibrate the shift of binding energy.

Electrochemical analyses. All samples were ground before preparing inks. Typically, 5 mg of catalyst was dispersed in 950 μL of isopropanol/water (1:2 in volume) mixed solvent. Then 50 μL of 5.0 wt% Nafion solution was added and the suspension was further sonicated for at least 30 min to obtain a homogenous catalyst ink. 5 μL of the catalyst ink was dropped on the glassy carbon (GC) electrode with a diameter of 4 mm (RRDE Pt Ring/GC Disk Electrode, ALS Co., Ltd.). The loading of catalysts was 0.2 mg cm^{-2}. Electrochemical analyses were performed with a CHI 842B electrochemical analyzer (CH Instrument, USA). The catalyst film coated RRDE was the working electrode. A Pt wire and the saturated calomel electrode (SCE) were used as counter electrode and reference electrode, respectively. Cyclic voltammetry (CV) and linear sweep voltammetry (LSV) measurements were conducted in O_2/N_2 saturated 0.1 M KOH solutions. The scan rate of CV and LSV were 50 and 10 mV s^{-1}, respectively. The rotating speed for LSV was 1600 rpm. According to the Nernst equation (E_{RHE}=E(SCE)+0.0591*pH+0.241), all potential values were normalized to the reversible hydrogen electrode (RHE) in this study. The current density was calculated based on the geometrical area (0.1256 cm^2) of GC electrode after the correction of double layer capacitance.

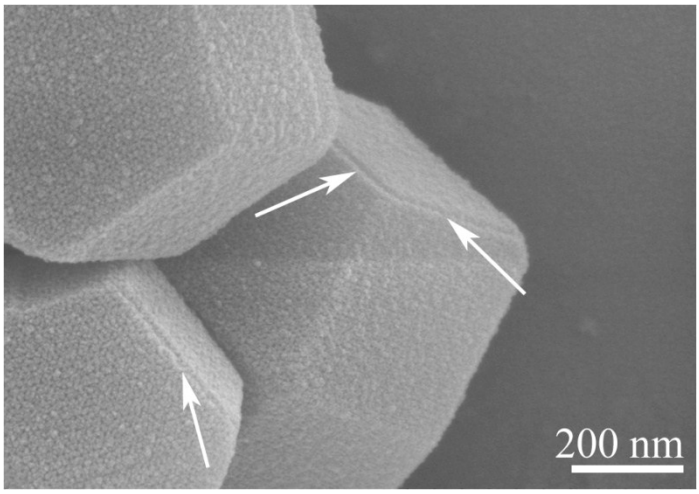

Fig. S1 SEM image of ordered mesoporous polymer (OMP) single-crystals with clear plate-like thin layers on their surfaces.

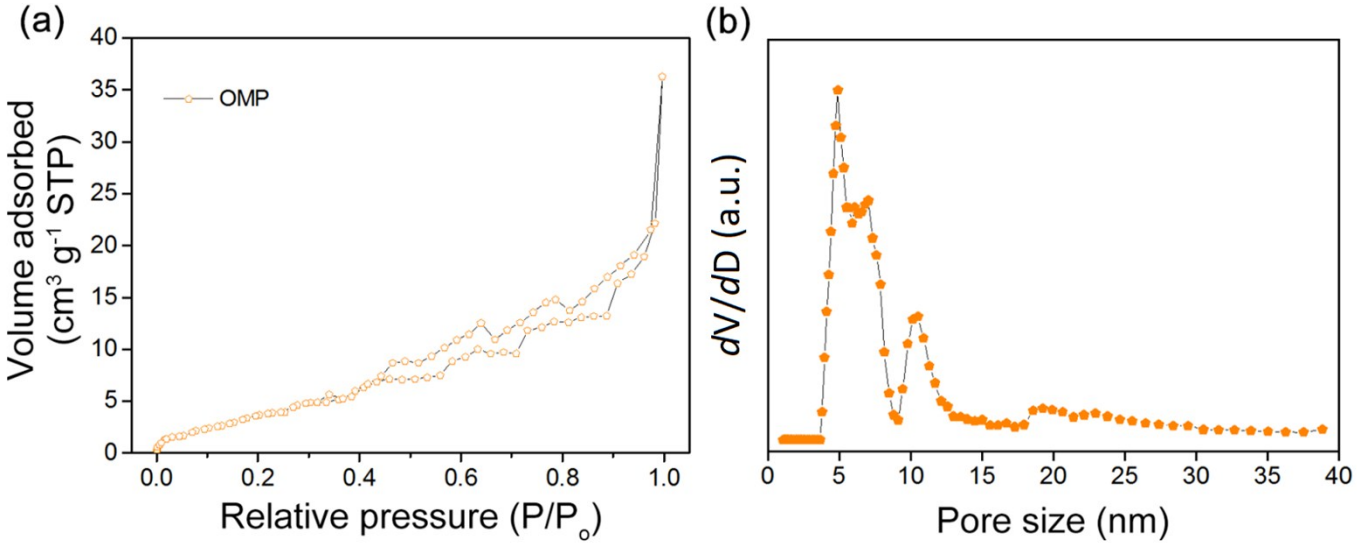

Fig. S2 (a) N_2 adsorption-desorption isotherms and (b) corresponding pore size distribution of OMP. The N_2 adsorption-desorption isotherm of OMP is not very smooth due to the quite low specific surface area of OMP (18.7 cm^2 g^{-1}).

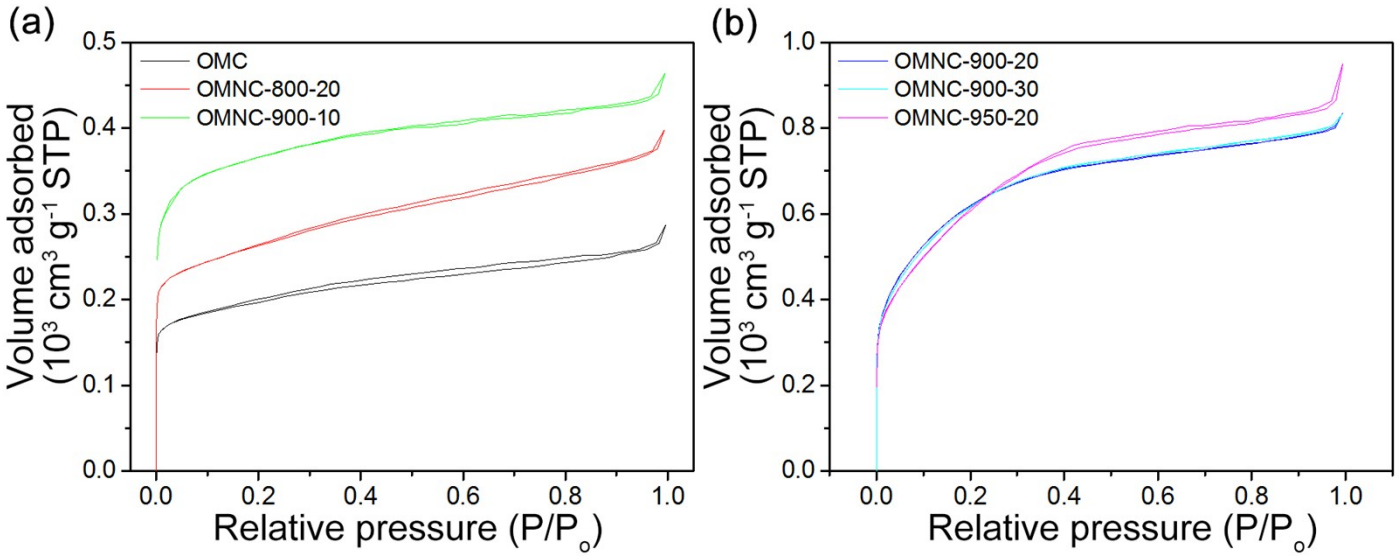

Fig. S3 N_2 adsorption-desorption isotherms of OMC and OMNC-*T*-*t*.

Note for Fig. S3: To clarify the N_2 adsorption-desorption isotherms of OMC and OMNC-*T*-*t* as shown in **Fig. 2b,** the isotherms are separated and put into two pictures as shown in **Fig. S3a** and **Fig. S3b.** The sharp N_2 uptakes in the low relative pressure region of $P/P_0 < 0.1$ can be attribute to the presence of micropores. The slow N_2 uptakes in the middle P/P_0 region from 0.2 to 0.9 are corresponding to the presence of mesopores. The hysteresis loops of the OMC and OMNC-*T*-*t* shown in **Fig. S3** is not quite obvious. It is known that the hysteresis loops of N_2 adsorption-desorption isotherms derived from the capillary condensation of nitrogen gas in mesopores are determined by pore sizes[S1-3] and temperatures.[S4] At a given temperature (77 K), the absence of hysteresis loop or inconspicuous hysteresis loop occurs when the mesopore size is less than or close to the critical pore size, [S5-7] regardless of cylindrical [S4, S8-10] and cage-like pores. [S11-14] Therefore, in the present study, such inconspicuous hysteresis loop shown in **Fig. S3** should be mainly attributed to the smaller mesopore size which is less than the critical pore size. Further, even when mesopores larger than the critical size exist, no hysteresis will be observed unless there is a percolation path from the surface in which all pores are supercritical. Otherwise the filling and emptying process is controlled by the narrow subritical pores that do not display hysteresis.

Upon increasing the NH_3 activation temperature and time, the total surface areas are gradually increased, and the hysteresis loops are gradually disappeared, such as OMNC-800-20, OMNC-900-10, OMNC-900-20, and OMNC-900-30 (**Fig. S3a** and **Fig. S3b**). The micropore ratios are gradually increased after higher and higher degree of NH_3 activation (**Table S1**). However, when the activation temperature and time increased to 950 °C and 20 min, respectively, the relative proportion of micropores are decreased from ~50 % to 28 %. The N_2 adsorption-desorption isotherm of OMNC-950-20 shows a small hysteresis loop again (**Fig. S3b**).

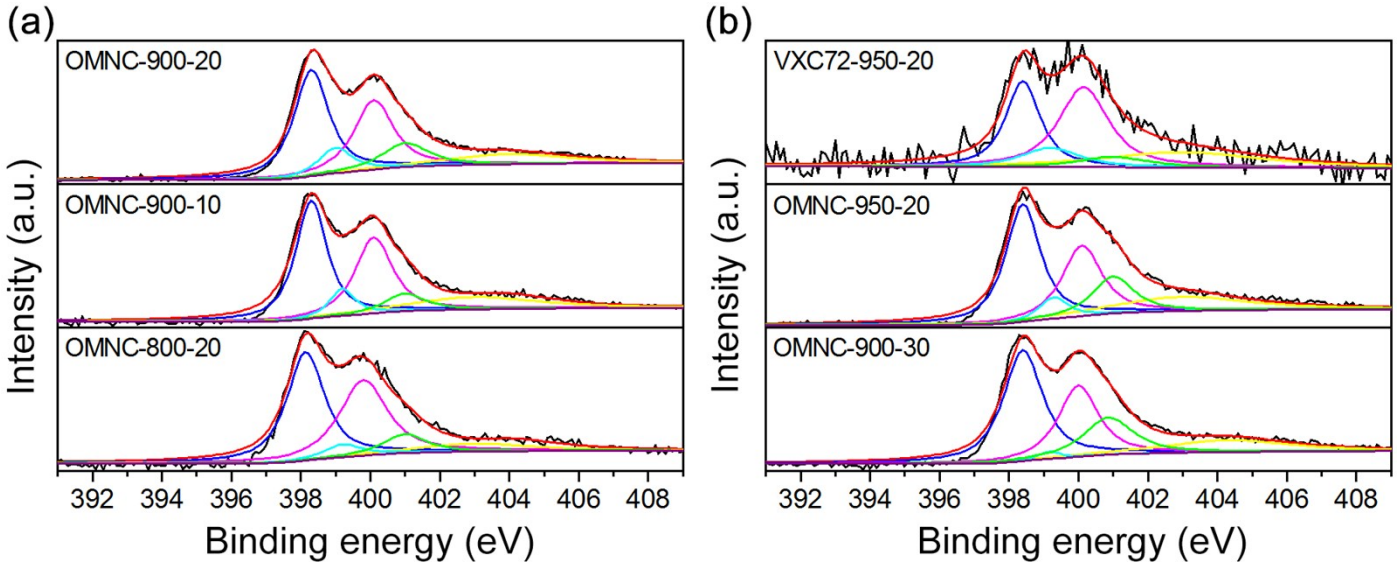

Fig. S4 High-resolution N 1s XPS spectra of OMNC-*T*-*t* and VXC-72-950-20.

Note for Fig. S4: To further clearly show the N 1s XPS spectra and fitting curves, **Fig. S3** reveals the same high-resolution N 1s XPS spectra of OMNC-*T*-*t* and VXC72-950-20 with two separated pictures: raw spectra (black), fitting curve (red), pyridinic N (blue), pyrolic N (pink), graphitic N (green), oxidized N (yellow), and amide or imine N (cyan).

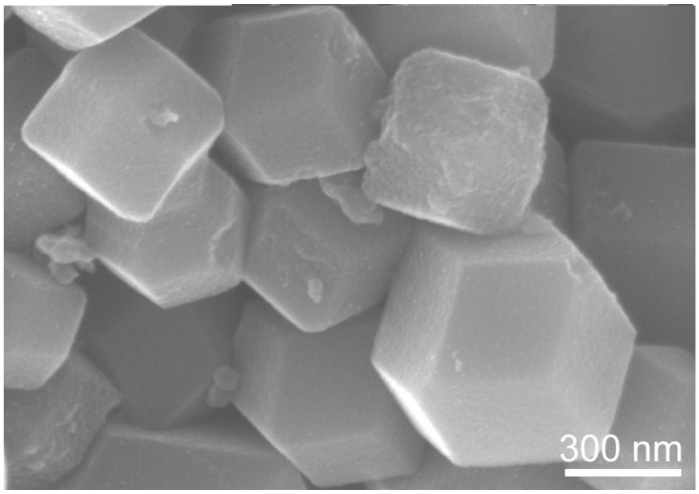

Fig. S5 SEM image of OMNC-950-20.

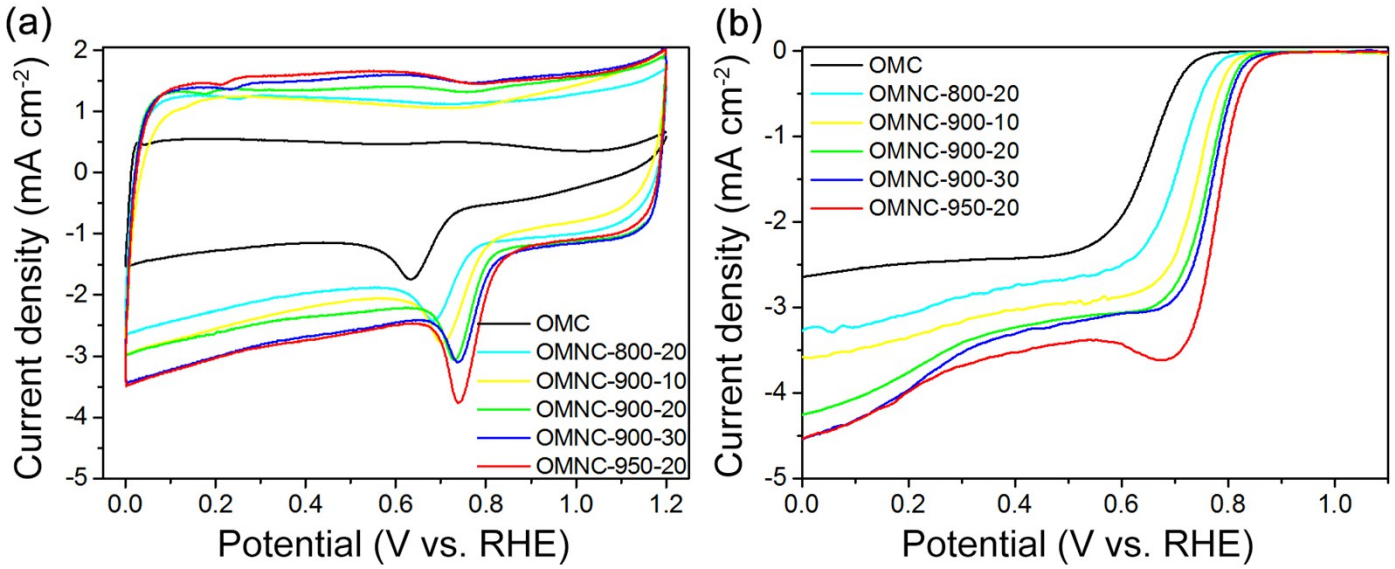

Fig. S6 (a) Cyclic voltammograms and (b) linear sweep voltammetry curves of OMC and OMNC-*T*-*t*.

Table S1 Physicochemical properties of the ordered mesoporous carbon (OMC) and ordered mesoporous nitrogen-doped carbon (OMNC).

Samples	d_{110} (nm)	S_{BET} ($m^2\ g^{-1}$)	S_{Micro} ($m^2\ g^{-1}$)	S_{Micro}/S_{BET}	V_{Pore} ($cm^3\ g^{-1}$)	V_{Micro} ($cm^3\ g^{-1}$)	V_{Micro}/V_{Pore}	Yield (wt%)
OMC	8.08	733.5	355.6	0.48	0.443	0.185	0.42	–
OMNC-800-20	8.04	965.0	570.6	0.60	0.615	0.235	0.39	95.7
OMNC-900-10	7.86	1386.8	989.2	0.71	0.718	0.392	0.55	73.8
OMNC-900-20	7.17	2252.4	1234.6	0.55	1.291	0.526	0.41	39.0
OMNC-900-30	6.96	2255.5	1158.4	0.51	1.305	0.489	0.37	34.1
OMNC-950-20	6.86	2250.0	617.5	0.28	1.468	0.244	0.17	15.9

d_{110}: Spacing of 110 planes; S_{BET}: Specific surface area; S_{Micro}: Micropore surface area; V_{Pore}: Pore volume; V_{Micro}: Micropore volume

Table S2 Total N content of OMNC-*T*-*t* and the relative content of three main types of N among all species based on the XPS analyses.

Samples	N content (at%)	Percentage (%)		
		Pyridinic N	Pyrrolic N	Graphitic N
OMNC-800-20	3.0	41.2	36.1	10.2
OMNC-900-10	4.4	43.7	25.3	10.8
OMNC-900-20	6.1	40.8	26.3	11.7
OMNC-900-30	5.6	41.0	26.3	17.2
OMNC-950-20	5.4	37.5	25.8	16.5
VXC72-950-20	0.7	27.0	36.5	7.5

References

S1 M. Kruk and M. Jaroniec, *Chem. Mater.*, 2000, **12**, 222-230.

S2 M. Kruk and M. Jaroniec, *Chem. Mater.*, 2003, **15**, 2942-2949.

S3 C. J. Rasmussen, A. Vishnyakov, M. Thommes, B. M. Smarsly, F. Kleitz and A. V. Neimark, *Langmuir*, 2010, **26**, 10147-10157.

S4 K. Morishige, N. Tateishi and S. Fukuma, *J. Phys. Chem. B*, 2003, **107**, 5177-5181.

S5. T. Allen, in *Particle Size Measurement*, Springer Netherlands, 1990, vol. 2, pp. 104-131.

S6 P. I. Ravikovitch and A. V. Neimark, in *Studies in Surface Science and Catalysis*, eds. A. Sayari and M. Jaroniec, Elsevier, 2000, vol. 129, pp. 597-606.

S7 J. Rathouský and M. Thommes, in *Studies in Surface Science and Catalysis*, eds. R. Xu, Z. Gao, J. Chen and W. Yan, Elsevier, 2007, vol. 170, pp. 1042-1047.

S8 H. Yang, Yan, Y. Liu, F. Zhang, R. Zhang, Y. YanMeng, M. Li, S. Xie, B. Tu and D. Zhao, *The J. Phys. Chem. B*, 2004, **108**, 17320-17328.

S9 Y. Meng, D. Gu, F. Zhang, Y. Shi, L. Cheng, D. Feng, Z. Wu, Z. Chen, Y. Wan, A. Stein and D. Zhao, *Chem. Mater.*, 2006, **18**, 4447-4464.

S10 M. Li and J. Xue, *J. Colloid Interface Sci.*, 2012, **377**, 169-175.

S11 F. Zhang, Y. Meng, D. Gu, Yan, C. Yu, B. Tu and D. Zhao, *J. Am. Chem. Soc.*, 2005, **127**, 13508-13509.

S12 F. Zhang, D. Gu, T. Yu, F. Zhang, S. Xie, L. Zhang, Y. Deng, Y. Wan, B. Tu and D. Zhao, *J. Am. Chem. Soc.*, 2007, **129**, 7746-7747.

S13 D. Gu, H. Bongard, Y. Meng, K. Miyasaka, O. Terasaki, F. Zhang, Y. Deng, Z. Wu, D. Feng, Y. Fang, B. Tu, F. Schüth and D. Zhao, *Chem. Mater.*, 2010, **22**, 4828-4833.

S14 F. Yin, G. Dong, Z. Ying, W. Zhangxiong, L. Fuyou, C. Renchao, D. Yonghui, T. Bo and Z. Dongyuan, *Angew. Chem. Int. Ed.*, 2010, **49**, 7987-7991.